Supporting information

1. Materials

$Ni(NO_3)_2 \cdot 6H_2O$, $Fe(NO_3)_3 \cdot 9H_2O$, o-phenylendiamine, polyacrylonitrile, salicylaldehyde and RuO_2 were purchased from Aladdin chemical reagent company. Nafion (5 wt %) were supplied by Alfa Aesar. All reagents were of analytical grade and were used as received.

2. Catalyst Characterization

The X-ray powder diffraction (XRD) patterns of the samples were obtained on a Shimadzu XRD-6000 diffractometer with Cu K_α radiation (λ=1.54178 Å). Scanning electron microscope (SEM) images were collected using a field-emission scanning electron microscope (JSM-6701F, FEOL). Transmission electron microscopy (TEM) images were taken with a JEM-2010 transmission electron microscope. The nitrogen adsorption-desorption characterization was performed with an ASAP2020 micrometrics instrument at 77 K. Autosorb-iQ2-MP nitrogen adsorption specific surface area analyzer was used to measure the specific surface area and pore size distribution of samples. The X-ray photoelectron spectroscopy (XPS) was obtained at a Thermo Fisher Scientific's K_α X-ray photoelectron spectrometer.

3. Electrochemical Measurements

3.1 For HER and OER

The electrochemical performance of the product was characterized by an electrochemical workstation CHI760E (CH Instrument, Shanghai, China). The electrochemical tests of HER and OER was carried out in a three-electrode system using Ag/AgCl (in 3.0 M KCl) as the reference electrode, a carbon rod as the counter electrode, and a glassy carbon (GC) electrode coated with the products as the working electrode. 1.0 M KOH was used as the electrolyte. The first step was the preparation of the working electrode. After the catalyst is thoroughly ground, 5 mg of the catalyst was dispersed in a mixed solution of water (100 μL), alcohol (400 μL), and Nafion solution (5 μL, 10 wt %) to form homogeneous ink via a continuous sonication treatment for 30 min. The working electrode was prepared by dripping 5.0 μl catalyst ink on the polished surface of the electrode, which was air-dried naturally to obtain a loading of 0.70 mg

cm^{-2}. For comparison purpose, electrocatalytic activity of commercial Pt/C (for HER comparison) and RuO_2 (for OER comparison) were evaluated when the loading was 0.70 mg cm^{-2} under the same conditions. The cyclic voltammetric (CV) pretreatment was arranged before other tests to activate the electrocatalysts and achieve a stable state of the material. The voltage range of the CV scan was 1.0-2.0 V (vs RHE); the scan rate was 50 mV s^{-1}. The linear sweep voltammetric (LSV) was measured at a scan rate of 10 mV s^{-1}, the overpotential (η) for HER can be calculated from a formula η = E (vs Ag/ AgCl) + 0.059 pH + 0.197 V. The overpotential (η) for OER can be calculated from a formula η = E (vs Ag/ AgCl) + 0.059 pH + 0.197 V - 1.23 V. Electrochemical impedance spectra (EIS) were recorded at 0.6 V vs Ag/AgCl in the frequency range 0.1-100 000 Hz with an amplitude of 10 mV.

3.2 *Determination of Electrochemical Capacitance*

The electrochemical surface area (ECSA) was estimated by CV scan in the non-faradaic potential range (0.4-0.45 V vs RHE) at different scan rates (5, 10, 15, 20, and 25 mV s^{-1}). By plotting the current density difference (Δj) between the anodic and cathodic current densities against the scan rate, the linear slope (i.e., twice of the double layer capacitance (C_{dl})) was used to represent ECSA.

3.3 *Turnover frequency (TOF) calculation*

In order to calculate the turnover frequency (TOF) of the surface active sites, CV test was performed with the potential range of -0.2 to 0.6 V (vs. RHE) at a scan rate of 50 mV s^{-1} to obtain the number of active sites in 1.0 M PBS (pH = 7). With a given geometric area A, the number of effective sites n is proportional to the charge Q, and the charge Q can be calculated from the obtained CV curve by integration. Therefore,

$$I_{cv} = J_{cv} \cdot A$$

$$t = \frac{U_{cv}}{v}$$

$$Q = \frac{1}{2}\int (I_{cv} t) = \frac{1}{2}\int d\left(\frac{U_{cv}}{v} J_{cv}\right) = \frac{1}{2}\int \frac{1}{v} d(U_{cv} J_{cv} A) = \frac{A}{2v}\int dU_{cv} J_{cv} = \frac{SA}{2v}$$

Because the charge Q of surface active sites (n) can be described by $Q = nF$,

59 therefore,

60 $$n = \frac{SA}{2vF}$$

61 Where I_{cv} , J_{cv} , U_{cv} are the current, current density, and potential obtained from CV
62 curve, v is the scan rate, and S is the integrated area of CV curve. When the number of
63 active sites is determined, the TOF (s^{-1}) was calculated with the equation:

64 $$\text{HER: TOF} = \frac{I}{2nF} = \frac{I}{2F}\frac{2vF}{SA} = \frac{vI}{SA} = \frac{Jv}{S}$$

65 $$\text{OER: TOF} = \frac{I}{4nF} = \frac{I}{4F}\frac{2vF}{SA} = \frac{vI}{2SA} = \frac{Jv}{2S}$$

66 where I is the current (in A) for different samples during the LSV measurements in
67 1.0 M KOH, J is the current density in LSV curves, v is the scan rate, F is the Faraday
68 constant (in $C\ mol^{-1}$), and n is the number of active sites (in mol) for different samples,
69 and S is the integrated areas of CV curves.

70 3.4 *For overall water splitting*

71 Preparation of electrode: 5 mg catalyst was ultrasonically dispersed into a mixture
72 of 100 μL ethanol and 400 μL distilled water until the dispersion was uniform. 350 μL
73 of catalyst was coated to two pieces of processed nickel foam (1×1 cm), respectively,
74 and dried naturally at room temperature for testing. For comparison purpose,
75 electrocatalytic activity of commercial Pt/C (for cathode) and RuO_2 (for anode) were
76 evaluated under the same conditions.

77

4. Results and Discussion

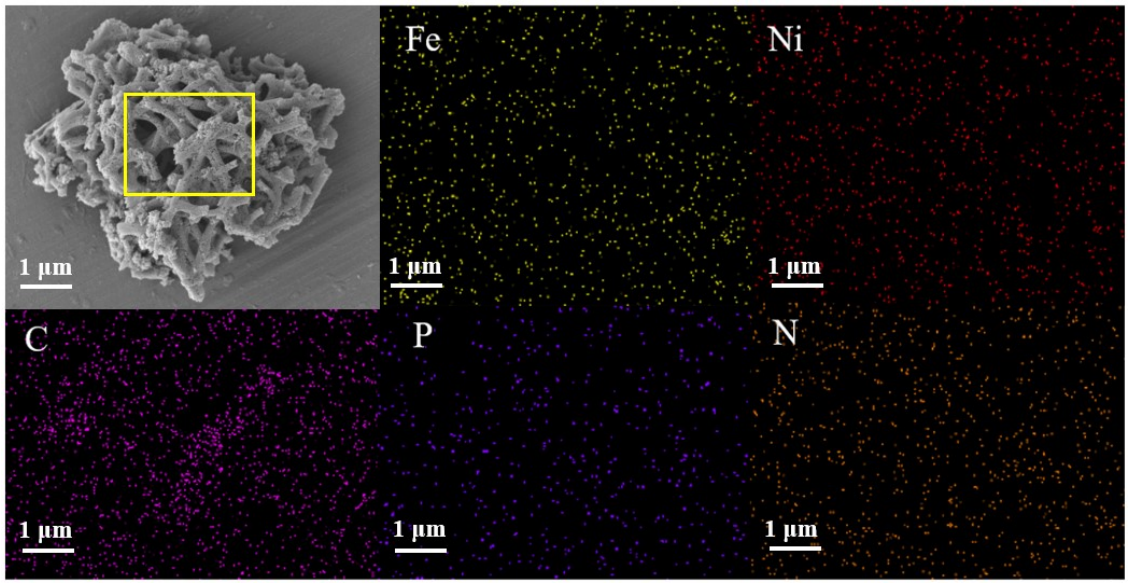

Fig. S1 SEM image and the selected area EDS mapping of the FNNP/NCF-1:3.

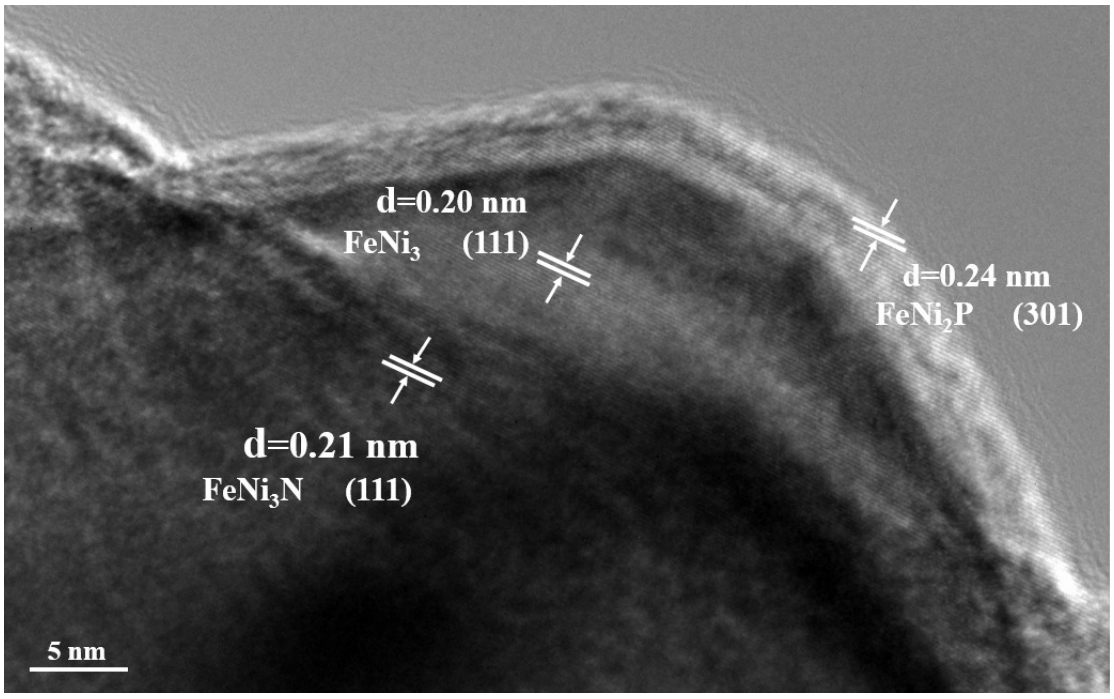

Fig. S2 The high-resolution TEM image of the FNNP/NCF-1:3.

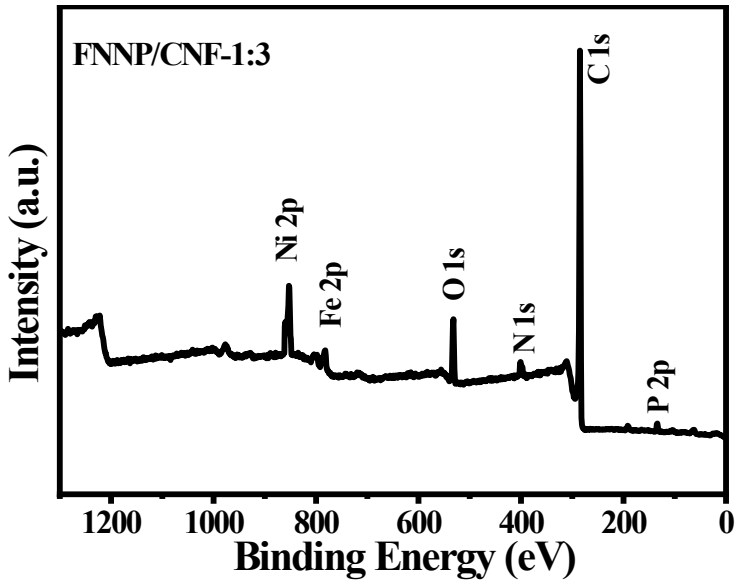

Fig. S3 The full survey XPS spectra of FNNP/NCF-1:3.

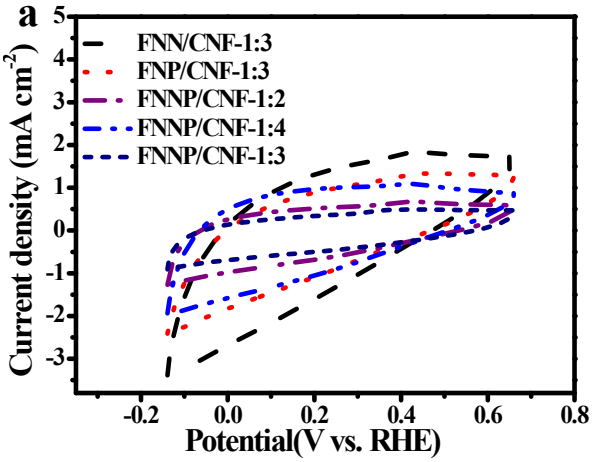

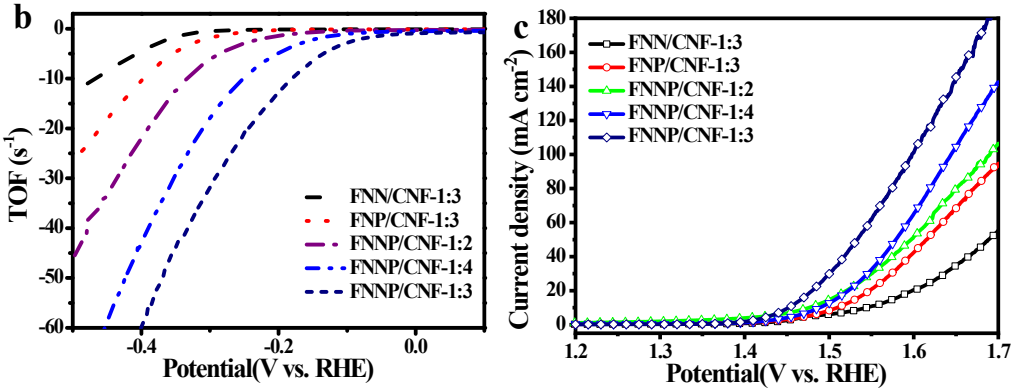

Fig. S4 (a) CV curves of the catalysts in 1.0 M PBS (pH=7) with a scan rate of 50 mV s^{-1}. TOF of the catalysts for HER (b) and OER (c) in 1.0 M KOH.

Table S1 Summary of Fe/Ni composite materials for HER in 1.0 M KOH.

Catalyst	Overpotential (mV) at 10 mA cm^{-2}	Overpotential (mV) at 100 mA cm^{-2}	Refs.
[a] P-$NiMo_4N_5$@Ni	178	307	Appl. Catal. B Environ. S0926-3373(18)30960-3.
[b] NiYCe-MOF/NF	197	387	Nano Lett. 2022, 22, 7238−7245
[c] Ni-Mo-Fe (NMF-6)	344	408	Int. J. Hydrogen. Energy. 46 (2021) 3821-3832.
[d] NiFe-LDH/$Ni(OH)_2$	157	275	Chem. Eng. J. 419 (2021) 129608
[e] $Ni(OH)_2$/NF	197	276	Sustain. Energ. Fuels. 2020, 4, 5031–5035
[f] Cu@Cu_3P/NF	218	302	Chem.Eur.J.2019,25,1083 –1089
[g] FeNi(BDC)(DMF,F)/NF	171	264	Appl. Catal. B Environ. 258 (2019) 118023
[h] P-rSWCNT	162	275	Appl. Catal. B Environ. 298 (2021) 120559
[i] α -CoNiOOH	190	270	Dalton T.49 (2020) 16962-16969.
FNN/NCF-1:3	128	352	This work

[a] Hydrothermal preparation of nickel foam loaded with nickel-molybdenum nitride after ammonification treatment.

[b] Preparation of nickel-yttrium cerium nickel foam loaded MOF by hydrothermal method.

[c] Nickel-iron hydroxide loaded on nickel foam, electrodeposited nickel-cobalt metal after carbonization.

[d] Electrodeposition of nickel-iron hydroxide followed by nickel hydroxide on nickel foam.

[e] Nickel foam heating loaded with nickel hydroxide.

[f] Nickel foam water bath heated to grow copper oxide, alkaline environment copper oxide reaction to copper hydroxide after phosphorylation.

[g] Black foam nickel hydrothermally loaded nickel-iron MOF

[h] $NaH_2PO_2 \cdot H_2O$ was used as phosphorylated SWCNT as a P source.

[i] Preparation of nickel-substituted α-$Co(OH)_2$ α-CoNiOOH sheets by co-precipitation.

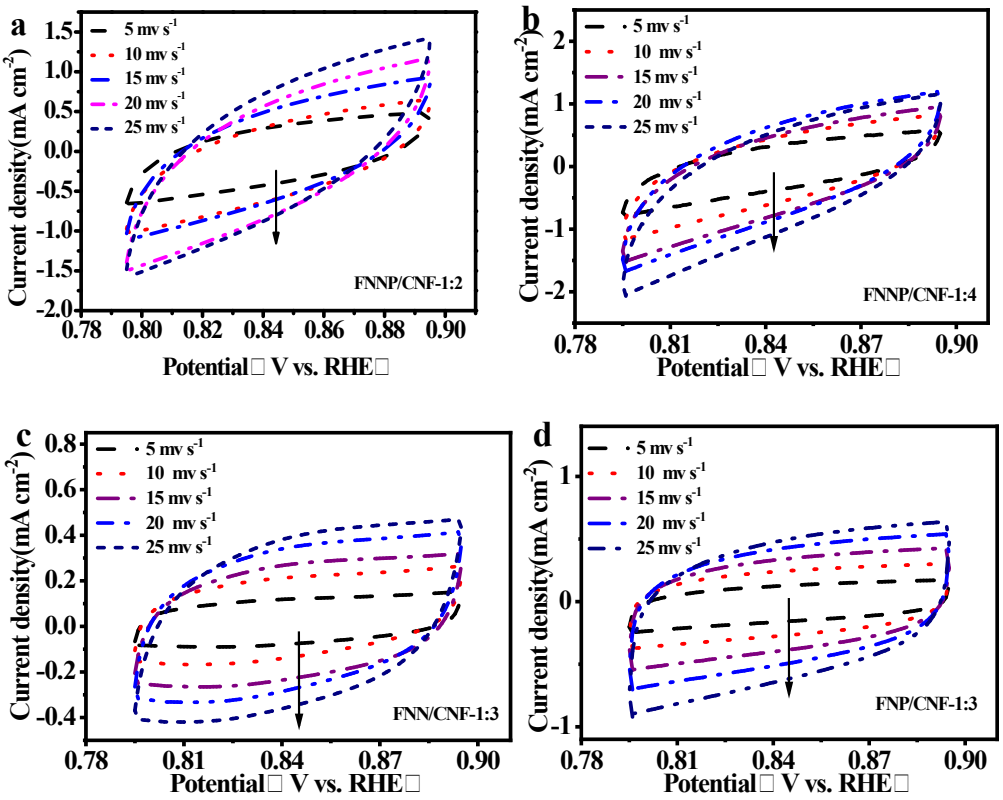

Fig. S5 The CV curves of (a)FNNP/CNF-1:2, (b) FNNP/CNF-1:4, (c) FNN/CNF-1:3, (d) FNP/CNF-1:3 in non-Faradaic potential range at different scan rates in 1.0 M KOH.

Table S2 Summary of Fe/Ni composite materials for OER in 1.0 M KOH.

Catalyst	Overpotential (mV) at 10 mA cm^{-2}	Overpotential (mV) at 100 mA cm^{-2}	Refs.
[a] CoNiMo-O/H_2-450	293	359	Chemelectrochem. 2018, 5, 1-9.
[b] H-Ni_2Fe_2N/Ni_3Fe@N-CS	236	351	Appl. Surf. Sci.566 (2021) 150706
[c] Ni/MoN@NCNT/CC	252	368	J. Alloy. Compd. 934 (2023) 167846.
[d] $Ni(OH)_2$@NiS_2	309	359	Chemelectrochem. 7 (2020) 745-752.
[e] NF/PANI/ NiFeeOH	170	340	Int. J. Hydrogen. Energy. 47 (2022) 34025 e34035
[f] NiFe NCs	281	305	J. Colloid. Interf. Sci. S0021-9797(18)31294-3
[g] Fe_2O_3/$Fe_{0.64}Ni_{0.36}$@Cs	274	368	Small 2023, 2208276
[h] Ni_3S_2/MIL-53(Fe)	214	251	Chemistryselect. 6 (2021) 1320-1327.
[i] Ru, Ni–CoP	251	360	Appl. Catal. B Environ. 298 (2021) 120488.
[j] Fe^{2+}-NiFe-LDH-EO6 h@ NF	239	285	ACS Sustain. Chem. Eng. 6 (2018) 11724-11733.
FNN/NCF-1:3	222	369	This work

[a] Hydrothermal loading of cobalt-nickel-molybdenum precursors with nickel foam followed by hydrogen reduction

[b] $Ni_3[Fe(CN)_6]_2$ PBAs were prepared by hydrothermal methodprecursors, and then $Ni_3[Fe(CN)_6]_2$ PBAs precursors were pyrolyzed to synthesize Ni-Fe nitrides and alloys.

[c] Growth of N-doped carbon nanotubes wrapped in Ni/MoN heterostructures on carbon cloth

[d] Preparation of $Ni(OH)_2$@NiS_2 heterostructures by reflux.

[e] Electrodeposition of nickel-iron hydroxide after electropolymerization of PANI on nickel foam.

[f] Room temperature synthesis of nickel-iron nanocube precursors, phosphorylated after pyrolysis.

[g] Room temperature synthesis of Schiff base solution followed by the addition of nickel-iron metal salt solvent thermal reaction to prepare nickel-iron alloy.

[h] NiFe foam-loaded Ni_3S_2/ MIL-53(Fe).

[i] PAN oxidation decomposition produces pores to fabricate porous ruthenium-nickel phosphide nanofibers.

[j] Growth on nickel foam Fe^{2+} -NiFe-LDH.

Table S3 Summary of Fe/Ni composite materials for overall water splitting in1.0 M KOH.

Catalyst	Cell voltage (mV) at 10 mA cm^{-2}	Refs.
[a] FeNiS-NF	1.54	Catalysts. 9 (2019) 597.
[b] $NiFe_2O_4$@N-rGO-CC	1.67	Energ. Fuel. 36 (2022) 4911-4923.
[c] NiFe-Pi/P	1.57	Appl. Surf. Sci. 598 (2022) 153717.
[d] $NC_{0.9}$ $F_{0.1}$ P HHAs	1.57	Electrochim. Acta. 334 (2020) 135633.
[e] Fe-CoP UNSs / NF	1.46	J. Mater. Chem. A 7 (2019) 20658-20666.
[f] FeNiMoP	1.50	Sustain. Energ. Fuels. 5 (2021) 5789-5797.
[g] Co/Fe/$Ni(OH)_2$	1.59	Appl. Surf. Sci. 528 (2020) 146972.
[h] Ni-Fe-P	1.66	Appl. Surf. Sci. 561 (2021) 150080.
[i] Ni-Fe/S	1.46	Vacuum. 181 (2020) 109661.
FNN/NCF-1:3	1.47	This work

[a] Nickel-iron sulfide with nickel foam loading.

[b] Carbon cloth-loaded $NiFe_2O_4$@N-rGO.

[c] Nickel foam loaded nickel-iron phosphide.

[d] Nickel foam loaded $NC_{0.9}$ $F_{0.1}$ P HHAs.

[e] Nickel foam loaded Iron-doped cobalt phosphide ultra-thin nanosheets.

[f] Trimetallic nickel-iron-molybdenum phosphides grown on nickel foam (NF).

[g] Cobalt (Co) and iron (Fe) doped nickel hydroxide (Ni) nanosheets formed on the surface of nickel foam.

[h] Layered nickel-iron-phosphide (Ni-Fe-P) nanosheets grown on nickel foam (NF).

[i] A loaded three-dimensional (3D) iron-doped nickel sulfide was prepared on nickel-iron foam.

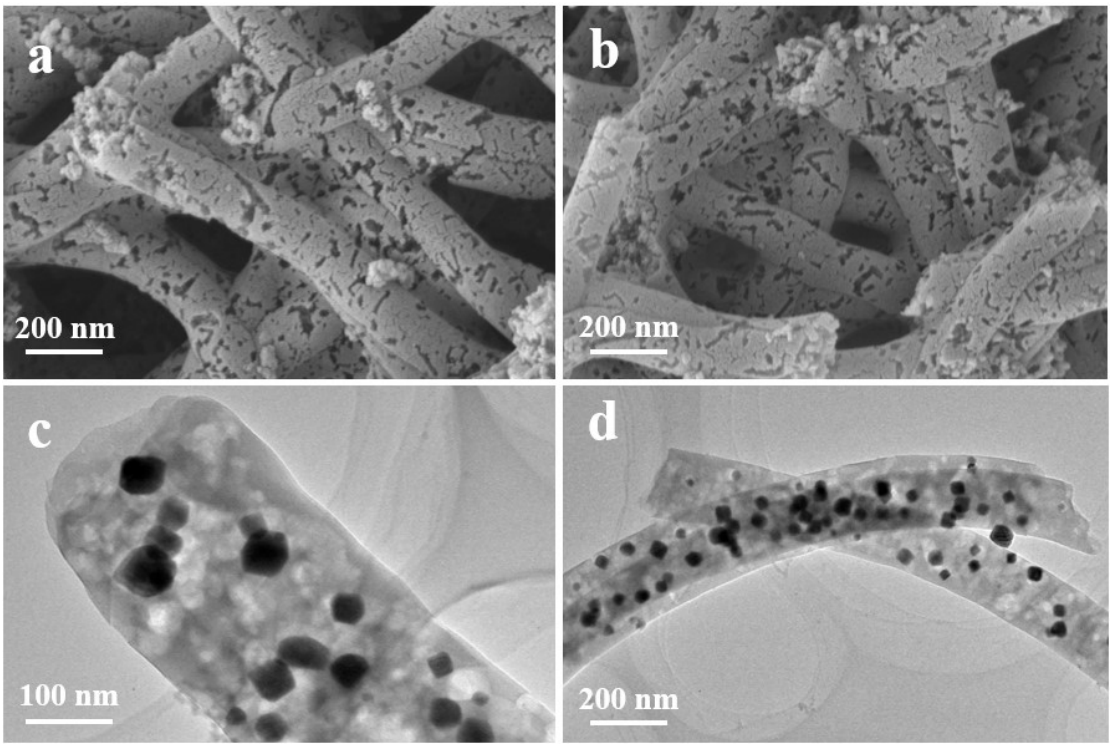

Fig. S6 (a) SEM image of FNNP/NCF-1:3 after HER cycle, (b) SEM image of FNNP/NCF-1:3 after OER cycle, (c) TEM image of FNNP/NCF-1:3 after HER cycle (d) TEM image of FNNP/NCF-1:3 after OER cycle.

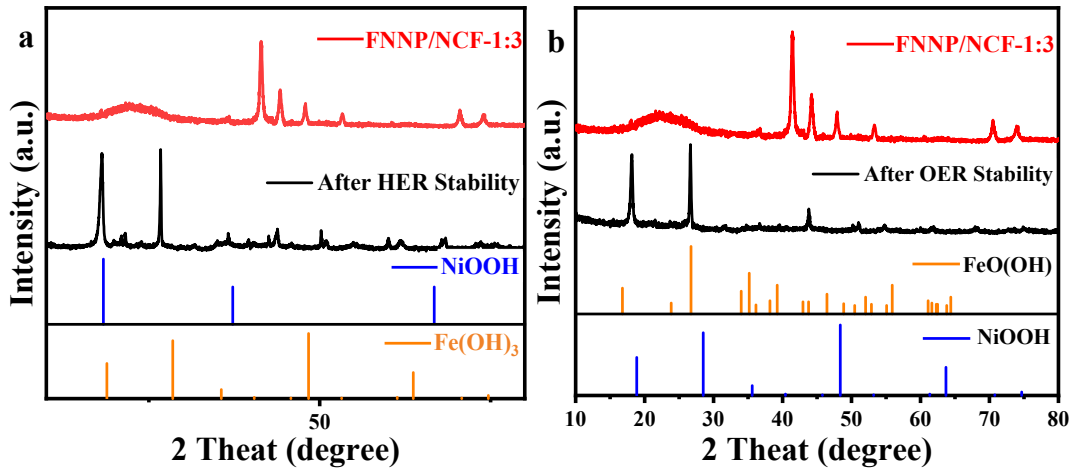

Fig. S7 Comparing XRD patterns of the FNNP/NCF-1:3 before and after (a) HER and (b) OER long-time tests.

156

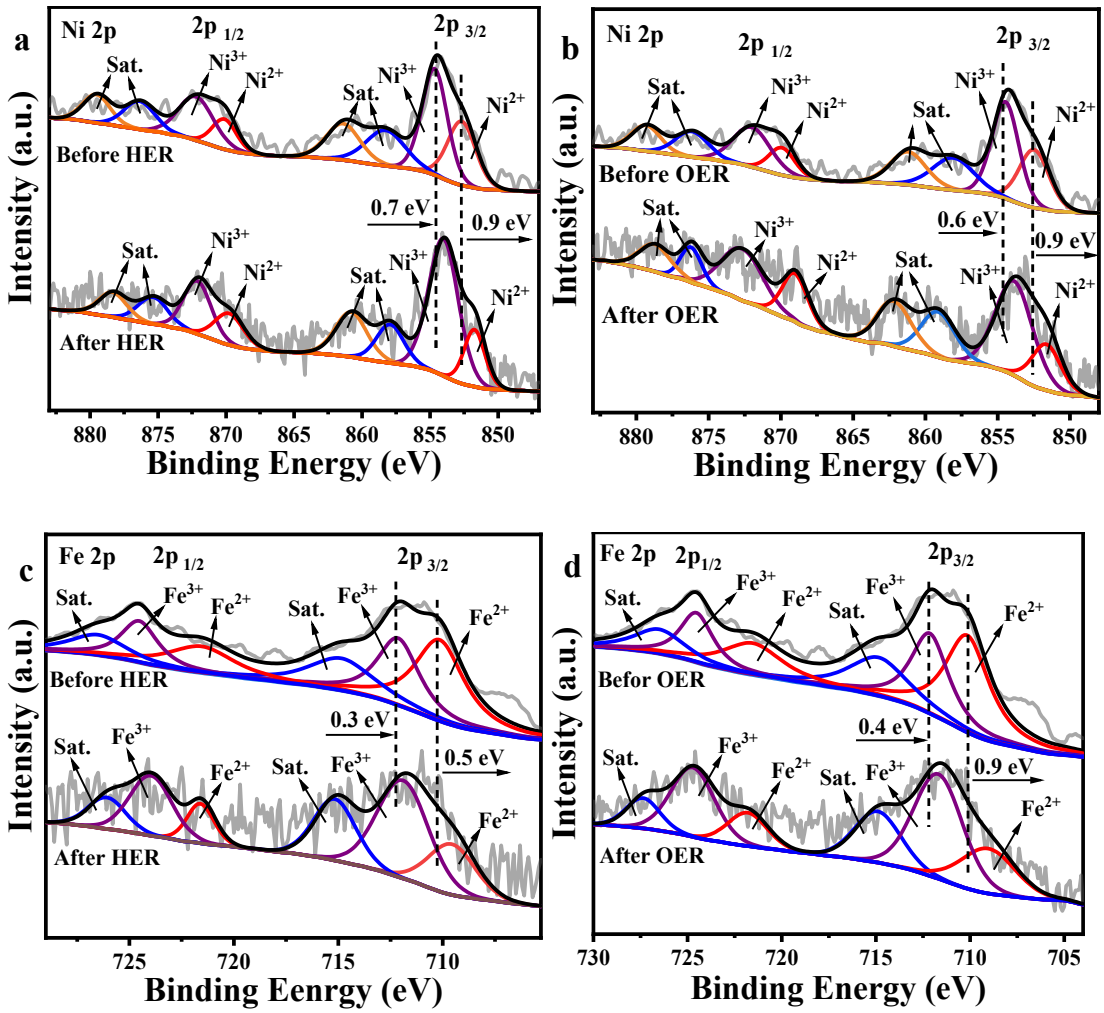

157

158

159 **Fig. S8** Comparing XPS spectra of (a-b) Ni 2p and (c-d) Fe 2p of patterns of the

160 FNNP/NCF-1:3 before and after HER and OER long-time tests.